THE JOURNAL OF BIOLOGICAL CHEMISTRY VOL. 284, NO. 40, pp. 27315–27326, October 2, 2009

A Novel Protein Associated with Membrane-type 1 Matrix Metalloproteinase Binds p27^{kip1} and Regulates RhoA Activation, Actin Remodeling, and Matrigel Invasion*[S]

Received for publication, July 5, 2009, and in revised form, August 2, 2009 Published, JBC Papers in Press, August 4, 2009, DOI 10.1074/jbc.M109.041400

Daisuke Hoshino, Taizo Tomari, Makoto Nagano, Naohiko Koshikawa, and Motoharu Seiki[1]

From the Division of Cancer Cell Research, Institute of Medical Science, University of Tokyo, Minato-ku, Tokyo 108-8639, Japan

Pericellular proteolysis by membrane-type 1 matrix metalloproteinase (MT1-MMP) plays a pivotal role in tumor cell invasion. Localization of MT1-MMP at the invasion front of cells, *e.g.* on lamellipodia and invadopodia, has to be regulated in coordination with reorganization of the actin cytoskeleton. However, little is known about how such invasion-related actin structures are regulated at the sites where MT1-MMP localizes. During analysis of MT1-MMP-associated proteins, we identified a heretofore uncharacterized protein. This protein, which we call p27RF-Rho, enhances activation of RhoA by releasing it from inhibition by p27^{kip1} and thereby regulates actin structures. p27^{kip1} is a well known cell cycle regulator in the nucleus. In contrast, cytoplasmic p27^{kip1} has been demonstrated to bind GDP-RhoA and inhibit GDP-GTP exchange mediated by guanine nucleotide exchange factors. p27RF-Rho binds p27^{kip1} and prevents p27^{kip1} from binding to RhoA, thereby freeing the latter for activation. Knockdown of p27RF-Rho expression renders cells resistant to RhoA activation stimuli, whereas overexpression of p27RF-Rho sensitizes cells to such stimulation. p27RF-Rho exhibits a punctate distribution in invasive human tumor cell lines. Stimulation of the cells with lysophosphatidic acid induces activation of RhoA and induces the formation of punctate actin structures within foci of p27RF-Rho localization. Some of the punctate actin structures co-localize with MT1-MMP and cortactin. Down-regulation of p27RF-Rho prevents both redistribution of actin into the punctate structures and tumor cell invasion. Thus, p27RF-Rho is a new potential target for cancer therapy development.

Malignant tumor cells grow invasively and form distant metastases after moving through multiple tissue barriers. Invasion requires cell locomotion together with degradation of the extracellular matrix (ECM)[2] by matrix metalloproteinases (MMPs) (1). MT1-MMP (MMP-14) is an integral membrane protease that degrades a variety of protein components within the extracellular milieu (2). The substrates of MT1-MMP include a variety of components of the ECM, membrane proteins including cell adhesion molecules, and growth factors and cytokines (3). To degrade the ECM barrier in advance of an invading cell, MT1-MMP localizes to the leading edge of invasion (4) and cellular protrusions called invadopodia (5–7). Therefore, it is of particular interest how reorganization of actin structures is regulated at sites where MT1-MMP localizes.

During mass spectrometric analysis of proteins co-purified with MT1-MMP, we identified a protein of unknown function (8). Although this protein did not affect MT1-MMP activity, we observed that enhanced expression or down-regulation of this protein affected activation of RhoA. Thus, we became interested in the possibility that this protein mediates focal reorganization of actin structures close to sites where MT1-MMP localizes.

RhoA plays a pivotal role in signal transduction pathways that regulate reorganization of actin structures and does so by assuming active GTP-bound and inactive GDP-bound states, with the transition between the two forms finely regulated by many cellular proteins (9, 10). In addition to the classical modulators, recent studies have revealed that p27^{kip1} also regulates activation of RhoA and Rac1 (11, 12). p27^{kip1} has been characterized as a cyclin-dependent kinase inhibitor localized to the nucleus, but phosphorylation of p27^{kip1} by protein kinase B/Akt or kinase-interacting stathmin (KIS) mediates its translocation from the nucleus to the cytoplasm. Cytoplasmic p27^{kip1} binds RhoA and prevents activation of RhoA by GEFs (12, 13). However, it is not known how inhibition of RhoA by p27^{kip1} is released to allow activation. The protein we identified binds p27^{kip1}, thereby preventing its binding to RhoA (schematically illustrated in supplemental Fig. S1). We named this protein p27RF-Rho (p27^{kip1} releasing factor from RhoA) based on this activity.

EXPERIMENTAL PROCEDURES

Plasmids—Complementary DNAs (cDNAs) encoding RhoGDI and CA-Lbc were gifts from Y. Takai (University of Osaka). cDNAs for p27RF-Rho, RhoA, p115RhoGEF, transferrin receptor, and p27^{kip1} were obtained from HT1080 cells by reverse transcription-PCR.

Cells and Culture Conditions—HT1080 and A375 cells were obtained from the American Type Culture Collection. HT1080

* This work was supported by a grant from the Specific Coordination Fund for Promoting Science (to D. H.), a grant-in-aid for Scientific Research on Priority Areas, "Integrative Research toward the Conquest of Cancer," and the Global COE Program from the Ministry of Education, Culture, Sports, Science, and Technology of Japan (to M. S.).

[S] The on-line version of this article (available at http://www.jbc.org) contains supplemental Figs. S1–S6.

[1] To whom correspondence should be addressed. Tel.: 81-3-5449-5255; Fax: 81-3-5449-5414; E-mail: mseiki@ims.u-tokyo.ac.jp.

[2] The abbreviations used are: ECM, extracellular matrix; MMP, metalloproteinase; MT1-MMP, membrane-type 1 MMP; FBS, fetal bovine serum; RBD, Rho binding domain; GST, glutathione *S*-transferase; GFP, green fluorescent protein; shRNA, short hairpin RNA; snRNA, small nuclear RNA; PBS, phosphate-buffered saline; RBD, Rho binding domain; LPA, lysophosphatidic acid; GEF, guanine nucleotide exchange factor; ROCK, Rho-associating coiled-coil containing kinase.

and A375 were maintained in Dulbecco's modified Eagle's medium containing 10% fetal bovine serum (FBS; Hyclone), 100 units/ml penicillin, and 100 μg/ml streptomycin (Invitrogen).

Antibodies and Chemicals—A polyclonal anti-p27RF-Rho antibody was prepared by immunizing a chicken with a recombinant protein expressed in *Escherichia coli*; the antibody obtained was affinity-purified. We used commercially available antibodies for Myc (Roche Applied Science), FLAG (Sigma), V5 (Invitrogen), GFP (Invitrogen), RhoA (Santa Cruz, sc-179), Cdc42 (BD Biosciences, 44), Rac (Upstate, 23A8), cortactin (Upstate, 4F11), glutathione *S*-transferase (GST; Cell Signaling, 26H1), and p27^{kip1} (Santa Cruz, c-19). AlexaFluor phalloidin was purchased from Molecular Probes. Y27632 (Calbiochem) was used at 10 μM, and cell-permeable C3 exoenzyme (Cytoskeleton) was used at 2 μg/ml. All other chemical reagents were purchased from Sigma-Aldrich or Wako unless otherwise indicated.

Knockdown Experiments Using shRNA and siRNA—The shRNA sequence used for knockdown of human p27RF-Rho was 5′-caccgtatgtcttcatagtcattgcgaacaatgactatgaagacatacc-3′. shRNA-expressing lentiviral vectors were generated and used according to the manufacturer's instructions. Three different siRNAs for human p27^{kip1} were designed, synthesized, and provided by B-bridge International: 5′-gugucuaacgggagcccua-3′, 5′-ggagcaaugcgcaggaaua-3′, and 5′-gaagguucauguagagaaa-3′. Cells were seeded and transfected with a 20 nM siRNA mixture (containing the three target sequences) using Lipofectamine™ RNAiMAX (Invitrogen), according to the manufacturer's instructions.

Preparation of Cytoplasmic and Membrane Fraction—Cells were disrupted under low osmotic conditions by resuspending the cells in 250 mM sucrose and 25 mM Tris-HCl (pH 7.5) containing protease inhibitor cocktail Set 1. After centrifugation at 6300 $\times$ *g* to remove nuclei and large cell debris, the supernatants were centrifuged again at 20,000 $\times$ *g* to pellet the membranes so that the supernatant represented the cytoplasmic fraction.

Co-immunoprecipitation and Pulldown Assays—HT1080 cells were lysed in immunoprecipitation buffer (1% Nonidet P-40, 50 mM Tris-HCl (pH 8.0), 150 mM NaCl, protease inhibitor mixture Set III). The beads were washed four times with immunoprecipitation buffer and eluted with FLAG peptides or Laemmli sample buffer.

The Pulldown Assay for Rho-GTPases—Cells were washed with ice-cold PBS, scraped off the plates in cell-lysis buffer (50 mM Tris-HCl (pH 7.4), 2 mM $MgCl_2$, 1% Nonidet P-40, 10% glycerol, 100 mM NaCl, supplemented with 1 mM dithiothreitol, 10 μg/ml leupeptin, 10 μg/ml aprotinin, and 10 μg/ml pepstatin-A) on ice. Lysates were centrifuged for 5 min at 20,000 $\times$ *g* at 4 °C. A fraction of the cleared lysates was incubated with 15 μg of GST-PAK-CRIB or GST-Rhotekin-Rho binding domain (RBD) bound to glutathione-coupled-Sepharose beads for 45 min at 4 °C. The pellet containing the beads was collected, washed 3 times with ice-cold cell lysis buffer, and subjected to SDS-PAGE followed by Western blot analysis using the indicated antibodies.

GST Pulldown Assay—Recombinant proteins such as GST, GST-RhoA, and GST-p27kip1 were expressed in *E. coli* BL21 Gold (DE3) pLysS (Stratagene) using the pDEST15 expression vector (Invitrogen). GST pulldown assays were performed as described previously (14).

Matrigel Invasion—Matrigel invasion assays were performed as described previously (15). Briefly, Transwells with 8-μm pore size filters (Corning) covered with Matrigel (BD Biosciences) were inserted into 24-well plates. Dulbecco's modified Eagle's medium (500 μl) containing 10% FBS was added to the lower chamber, and 200 μl of a cell suspension (5×10^4 cells) was placed in the upper chamber. The plates were incubated at 37 °C in a 5% CO_2 atmosphere for 6 h. Cells in the lower chamber were then stained with Giemsa solution and counted.

Fluorescent Gelatin Degradation Assay—Oregon Green-labeled gelatin was obtained from Invitrogen. Coverslips were coated with 50 μg/ml poly-L-lysine for 20 min at room temperature, washed with PBS, and fixed with 0.5% glutaraldehyde (Sigma) for 15 min. After 3 washes, 0.2% fluorescently labeled gelatin in 2% sucrose in PBS was incubated for 10 min at room temperature. After washing with PBS, coverslips were incubated in 5 mg/ml sodium borohydride for 3 min, washed 3 times in PBS, and finally incubated in 2 ml of complete medium for 2 h. To assess the ability of cells to form invadopodia and degrade the gelatin, cells were plated on Oregon Green-coated coverslips and incubated at 37 °C for 2 h.

Immunofluorescence Microscopy—Cells were fixed with 4% paraformaldehyde and permeabilized using 0.1% Triton-X100 in PBS for 10 min. After the cells were blocked in PBS containing 5% goat serum and 3% bovine serum albumin, they were incubated with primary antibodies. All primary antibodies were visualized with either an Alexa546-conjugated goat anti-mouse antibody (Invitrogen) or HiLyteFluor 647- or 488-conjugated goat anti-mouse or anti-chicken antibodies (AnaSpec). Cells were stained for F-actin using Alexa488- or 647-conjugated phalloidin (Invitrogen). Images of cells were captured with a Radiance 2100 microscope fitted with a confocal detection (Bio-Rad) or IX70 equipped with a CCD camera (Olympus).

Statistical Analysis—Data are represented as mean $\pm$ S.D. The unpaired Student's *t* test was used for analyzing differences between experimental groups.

RESULTS

p27RF-Rho Is Encoded by a Unique Gene Conserved in Vertebrates and Expressed Ubiquitously in Different Tissues—p27RF-Rho is a protein co-purified with MT1-MMP from a lysate of human melanoma A375 cells (8). This protein is composed of 161 amino acids encoded by an as yet uncharacterized gene (accession no. NM_017907). Gene orthologues for p27RF-Rho exist in vertebrates only as a single copy in each species, and the amino acid sequences are well conserved (supplemental Fig. S2*B*). p27RF-Rho does not have a signal sequence for secretion or other known protein motifs except for consensus sequences for myristoylation and palmitoylation at the N terminus (NH_2-MGCCY). Protein motifs of p27RF-Rho and its expression constructs are presented in Fig. 1*A*. Expression of the mRNA for p27RF-Rho was detected in almost all human tissues tested (supplemental Fig. S2*A*).

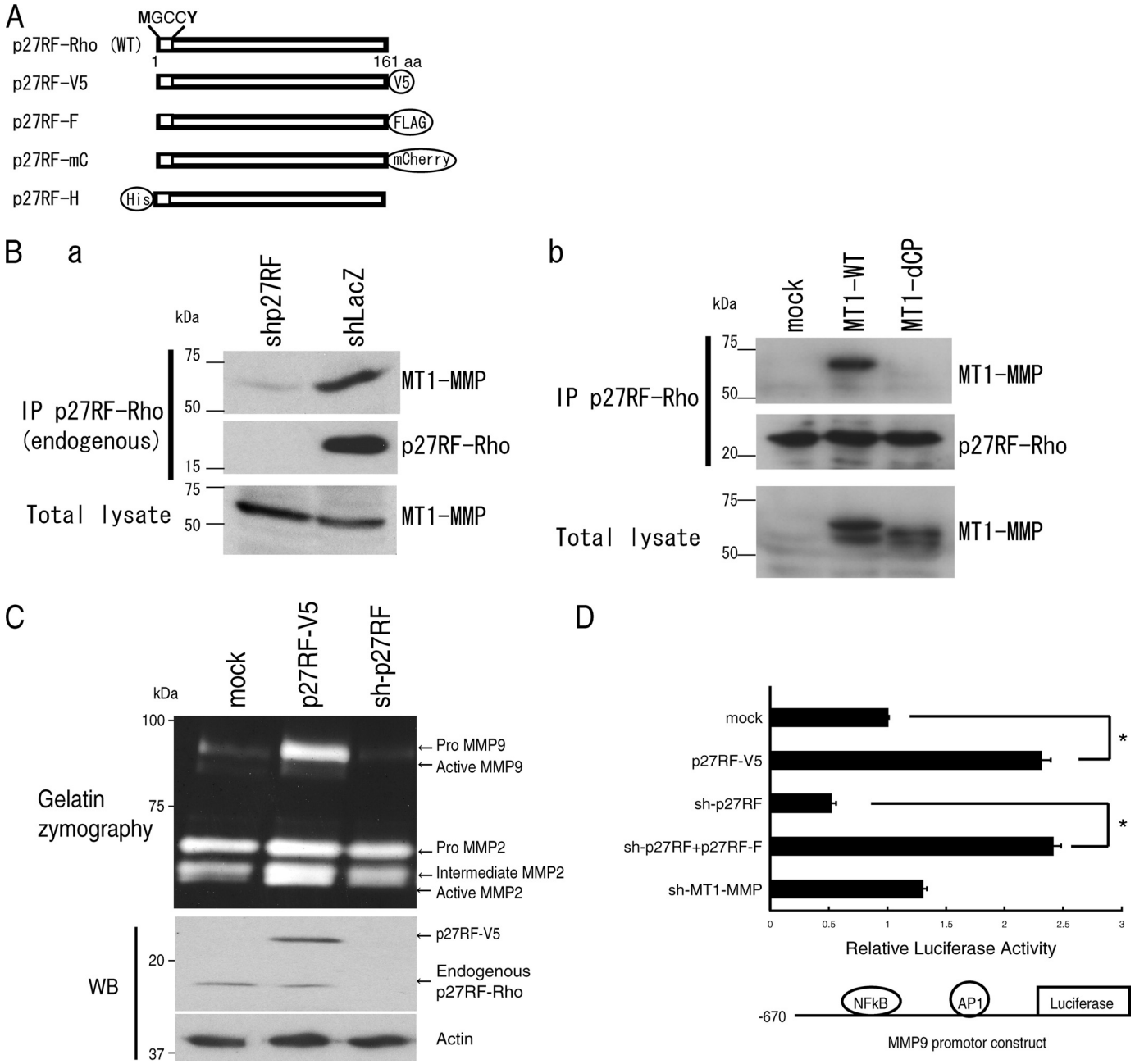

FIGURE 1. **The MT1-MMP-associating protein, p27RF-Rho, regulates expression of MMP-9.** *A*, schematic representation of p27RF-Rho and its tagged protein derivatives. p27RF-Rho has consensus sequences for myristoylation and palmitoylation at the N terminus as indicated. *p27RF-V5*, V5-tagged p27RF-Rho; *p27RF-F*, FLAG-tagged protein; *p27RF-mC*, mCherry-tagged protein including a truncation of the 3′-non-coding region of the p27RF mRNA so as to eliminate the sequence targeted by the shRNA for the knockdown experiments; *p27RF-H*, His-tagged protein. *B*, *a*, immunoprecipitation (*IP*) of endogenous p27RF-Rho by an anti-p27RF-Rho antibody co-precipitated endogenous MT1-MMP as detected by Western blot analysis of the immunoprecipitates using an anti-MT1-MMP antibody. *b*, p27RF-Rho-FLAG was expressed together with myc-MT1-MMP in HT1080 cells. p27RF-Rho was immunoprecipitated using an anti-FLAG antibody. Proteins bound to the antibody were eluted with FLAG peptides and subjected to Western blot analysis using an anti-Myc antibody. p27RF-Rho precipitated MT1-MMP but not a mutant MT1-MMP lacking the cytoplasmic tail. *C*, effect of p27RF-Rho on production of gelatinases was analyzed by gelatin zymography. Expression of p27RF-Rho in HT1080 cells was modulated by transfecting an expression plasmid for p27RF-V5, or endogenous protein expression was down-regulated using shRNA (*sh-p27RF*), respectively. Gelatinase activities of MMP-2 and MMP-9 secreted into the culture media were analyzed by gelatin zymography (*upper panel*). p27RF-Rho expression was analyzed by Western blot analysis (*WB*; *bottom panels*). *D*, the effect of p27RF-Rho on the *mmp-9* promoter was monitored using a luciferase reporter assay in HT 1080. The reporter construct is illustrated at the *bottom*. Data are shown as the mean ± S.D., $n = 5$. *, $p < 0.05$.

Specific Interaction of p27RF-Rho with MT1-MMP Does Not Affect MMP-2 Activating Activity—Because p27RF-Rho was identified as a protein co-purified with MT1-MMP, we tested whether p27RF-Rho indeed associates with MT1-MMP in HT1080 cells. Immunoprecipitation of endogenous p27RF-Rho precipitated a 17-kDa protein, and coprecipitation of endogenous MT1-MMP was detected by Western blot analysis (Fig. 1*B*, *a*). This interaction was also observed with exogenously expressed FLAG-tagged p27RF-Rho and Myc-tagged MT1-MMP (Fig. 1*B*, *b*). MT1-MMP has a short cytoplasmic tail comprising 20 amino acids. A mutant MT1-MMP lacking the cytoplasmic tail (MT1-dCP) did not co-precipitate with p27RF-

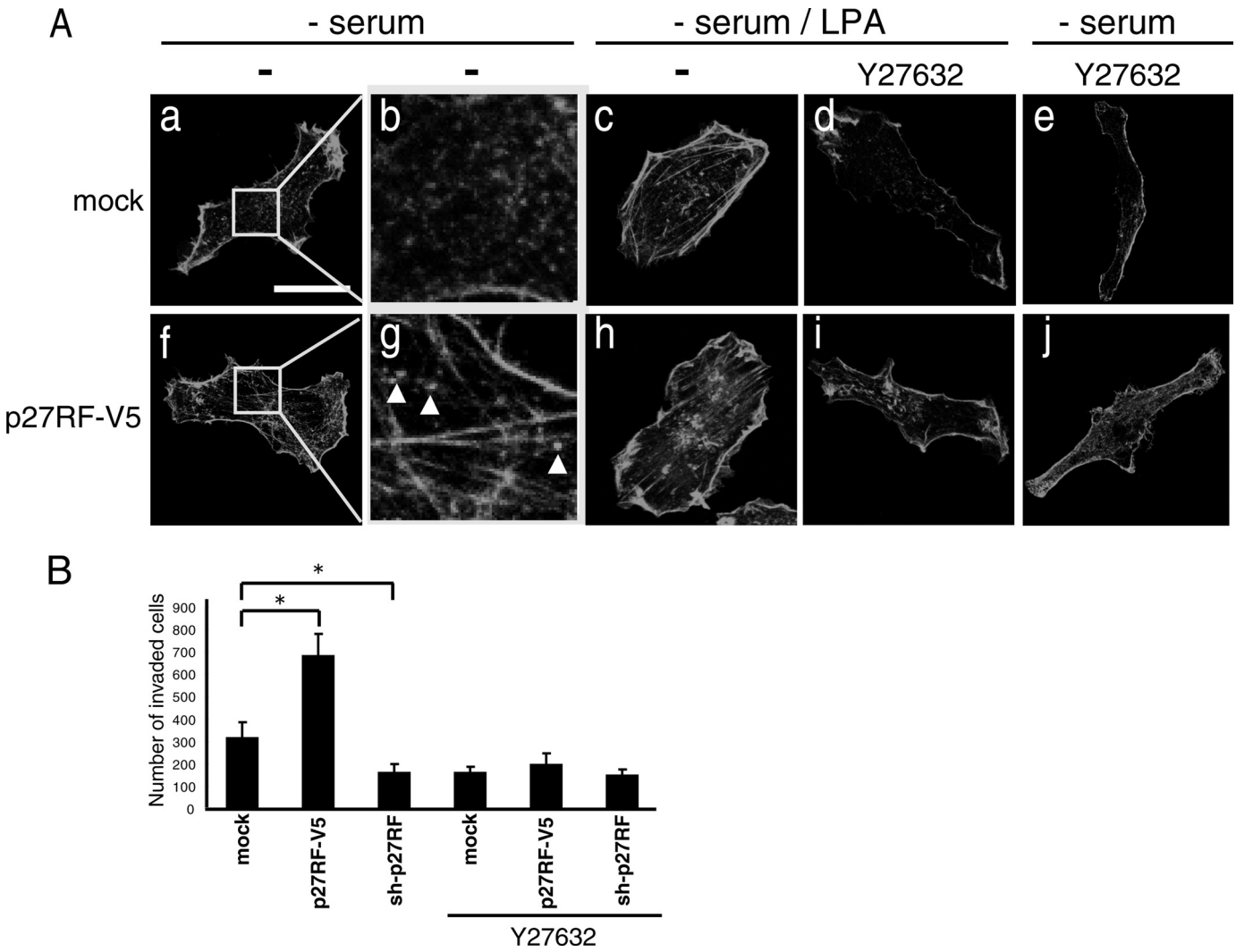

FIGURE 2. **p27RF-Rho modulates cell morphology via RhoA activity.** *A*, HT1080 cells stably expressing p27RF-V5 and mock cells (empty vector) were seeded onto collagen coated glass coverslips and treated with LPA and/or Y27632. Actin was visualized with Alexa488-phalloidin. Confocal images were performed using a 63× objective lens (*scale bar*, 20 μm). *B*, invasion of Matrigel was analyzed using the indicated HT1080 cell transfectants in the presence or absence of Y27632. The number of cells that had invaded through the Matrigel layer was counted. Data are shown as the mean ± S.D. ($n = 3$). *, $p < 0.05$ (Student's *t* test).

Rho, suggesting the importance of the cytoplasmic tail for this association (Fig. 1*B*, *b*). However, we have not detected direct binding between purified p27RF-Rho and the cytoplasmic tail peptide *in vitro* (data not shown). Thus, the interaction between p27RF-Rho and MT1-MMP may be indirect or may require other components.

p27RF-Rho may modulate the proteolytic activity of MT1-MMP through this interaction. To test this possibility, we analyzed the effect of p27RF-Rho on the ability of MT1-MMP to activate proMMP-2 in HT1080 cells (15). Neither forced expression of p27RF-Rho nor its down-regulation by expression of a specific shRNA had any obvious effect on MMP-2 activation (intermediate + active MMP-2 *versus* proMMP-2) (Fig. 1*C*). Unexpectedly however, forced expression of p27RF-Rho led to increased expression of MMP-9, and p27RF-Rho gene silencing led to decreased expression of MMP-9 (Fig. 1*C*). This effect of p27RF-Rho on MMP-9 expression was reproduced using a reporter gene construct comprising the *mmp-9* gene promoter, driving expression of the luciferase gene (Fig. 1*D*). Expression of p27RF-Rho enhanced reporter gene activity, and knockdown of endogenous p27RF-Rho inhibited this activity. In contrast, knockdown of MT1-MMP expression did not affect reporter gene activity, indicating that MT1-MMP does not regulate the p27RF-Rho activity to regulate mm-9 promoter.

Expression of p27RF-Rho Modulates Cell Morphology Regulated by RhoA—Upon expression of p27RF-Rho (p27RF-V5) in HT1080 cells, we noticed changes in cell morphology. To confirm this further, we visualized the actin cytoskeleton using Alexa488-phalloidin. Expression of p27RF-V5 in HT1080 cells enhanced formation of actin stress fibers (Fig. 2*A*, *f* and *g*). Expression of an empty vector did not affect the actin structure of the cells (Fig. 2*A*, *a* and *b*, *mock*). Weak, punctate expression of actin was observed in the control cells (Fig. 2*A*, *b*), whereas stronger and more dense punctate expression became obvious in the cells expressing p27RF-V5 (Fig. 2*A*, *g*, *white arrows*). RhoA regulates actin polymerization via an mDia-mediated pathway and actin depolymerization via a ROCK-mediated pathway (16, 17). To examine whether p27RF-V5 affects the actin cytoskeleton via activation of RhoA, we treated cells with

Y27632, which is a synthetic inhibitor of ROCK (17). Lysophosphatidic acid (LPA), an inducer of RhoA activation, stimulated the formation of stress fibers in the cells (Fig. 2*A*, *c* and *h*; *mock* and *p27RF-V5 panels*, respectively), and this effect was inhibited by Y27632 in both the control cells (Fig. 2*A*, *d*) and the p27RF-V5-expressing cells (Fig. 2*A*, *i*). We also observed that Y27632 inhibited formation of actin stress fibers in the cells expressing p27RF-V5 even in the absence of LPA stimulation (Fig. 2*A*, *j*). Thus, p27RF-V5 appears to affect RhoA activation and eventually stimulates the formation of stress fibers. Expression of p27RF-Rho also enhanced invasion of HT1080 cells into the reconstituted basement membrane called Matrigel (Fig. 2*B*, *p27RF-V5*). In contrast, knockdown of endogenous p27RF-Rho using shRNA inhibited invasion (Fig. 2*B*, *sh-p27RF*). Enhanced invasion by the expression of p27RF-V5 was prevented by exposure of the cells to Y27632 (Fig. 2*B*, *p27RF-V5+Y27632*). The cells used for the experiments are stable lines expressing each construct (refer to Fig. 3*A*, *a* for protein expression, *third panel* from the *top*).

It is also known that Rho/ROCK signaling stimulates expression of the *mmp-9* gene (20, 21). Indeed, the promoter activity enhanced by p27RF-Rho expression, as was observed in Fig. 1*D*, was suppressed by the C3 inhibitor of Rho subfamily proteins (supplemental Fig. S3*B*).

We also analyzed human malignant melanoma A375 cells whose round cell morphology is reported to be maintained by active Rho/ROCK signaling. Disruption of this signaling alters cell morphology, leading to the induction of multiple protrusions (18, 19). Indeed, the cells showed a typical round morphology when cultured on Matrigel/collagen-coated glass slides (supplemental Fig. S4*A*, *a*), and treatment of the cells with Y27632 reproduced the reported morphology with protrusions (supplemental Fig. S4*A*, *b*). Knockdown of endogenous p27RF-Rho by expressing shRNA induced a morphological change similar to that observed after treatment of the cells with Y27632 (supplemental Fig. S4*A*, *c*; for knockdown efficiency, refer to supplemental Fig. S4*B*).

p27RF-Rho Increases GTP-loaded RhoA—Because p27RF-Rho appeared to affect RhoA activity, we tested whether the amount of GTP-loaded RhoA in HT1080 cells is affected by p27RF-Rho (Fig. 2*A*). To measure this we used a recombinant fragment of the RBD of Rhotekin, a specific effecter of GTP-loaded Rho subfamily proteins (RhoA, -B, and -C). The expression of p27RF-V5 increased the amount of GTP-RhoA to 150% of the control value, whereas expression of sh-p27RF decreased the level of GTP-RhoA to 40% that of the control value (Fig. 3*A*, *a*, a representative Western blot; Fig.2*A*, *b*, quantification of the bands). Expression of p27RF-mC (Fig. 1*A*), which lacks the target sequence of sh-27RF in the 3′ non-coding region, in the knockdown cells reversed the effect of sh-p27RF expression, giving rise to a level of GTP-RhoA that was 90% that observed in the control cells (Fig. 3*A*, *b*). In contrast, GTP loading onto Rac1 or Cdc42 was unaffected by the expression of p27RF-V5 or knockdown of endogenous p27RF-Rho by shRNA (supplemental Fig. S6, *A* and *B*). p27RF-Rho does not affect the interaction between GTP-RhoA and Rhotekin RBD as demonstrated by an experiment using Rhotekin RBD and constitutively active RhoA (supplemental Fig. S6*C*).

Next we tested whether p27RF-Rho increases the binding of RhoA to GEFs that mediate GTP loading (Fig. 3*B*). We expressed Myc-RhoA in HT1080 cells together with p115-RhoGEF or constitutively active Lbc (CA-Lbc) and then immunoprecipitated Myc-RhoA and detected the GEFs in the precipitates by Western blot analysis. Expression of p27RF-V5 enhanced the binding of Myc-RhoA to p115-RhoGEF (Fig. 3*B*, *a*, *p27RF-V5* in the *top panel*; for quantification, see Fig. 3*B*, *b*). Conversely, down-regulation of endogenous p27RF-Rho with sh-p27RF decreased the binding of Myc-RhoA to the GEF (Fig. 3*B*, *a* and *b*, *sh-p27RF*). Similar results were obtained for another GEF protein, a constitutively active Lbc fragment (supplemental Fig. S6*D*, *CA-Lbc*). Taken together the results indicate that p27RF-Rho affects activation of RhoA by increasing interaction with GEFs.

p27RF-Rho Negates Inhibition of RhoA by p27^{kip1}—Accessibility of GEFs to RhoA is negatively regulated by Rho inhibitors that bind RhoA and prevent binding of GEFs. These include RhoGDIs (22) and the cytoplasmic form of p27^{kip1} (12). Because overexpression of p27RF-Rho increases binding of GEFs to RhoA, we tested whether p27RF-Rho interacts with RhoA inhibitors and whether it affects their function. FLAG-tagged p27RF-Rho (Fig. 1*A*, *p27RF-F*) was co-expressed with a GFP-fused form of RhoGDI-1 (GFP-RhoGDI) or p27^{kip1} (GFP-p27^{kip1}) in HT1080 cells and subjected to immunoprecipitation assay to determine whether p27RF-F co-precipitates with either or both RhoA inhibitors. Detection of the two RhoA inhibitors was carried out by Western blot analysis using anti-GFP antibody. Both GFP-tagged proteins were expressed at similar levels and were of similar molecular weights (Fig. 3*C*, *bottom panel*), but only GFP-p27^{kip1} co-precipitated with p27RF-F (Fig. 3*C*, *top panel*). To confirm the binding between p27RF-Rho and p27^{kip1} further *in vitro*, we expressed the following proteins in *E. coli* and purified them: His-tagged p27RF-Rho (Fig. 1*A*, *p27RF-H*), and GST-fused forms of RhoA and p27^{kip1} (supplemental Fig. S5*A*). p27RF-H bound GST-p27^{kip1} but not GST-RhoA (supplemental Fig. S5*B*).

Next, we examined whether p27RF-Rho affects the interaction between p27^{kip1} and RhoA *in vivo* (Fig. 3*D*). p27^{kip1} expressed in HT1080 cells was subjected to immunoprecipitation, and co-precipitation of RhoA was detected by Western blot analysis (Fig. 3*D*, *mock* in the *top panel*). Overexpression of p27RF-V5 in the cells decreased the amount of RhoA bound to p27^{kip1} (Fig. 3*D*, *p27RF-V5* in the *top panel*). Conversely, down-regulation of endogenous p27RF-Rho using shRNA increased the amount of RhoA bound to p27^{kip1} (Fig. 3*D*, *sh-p27RF* in the *top panel*). Thus, p27RF-Rho inhibits the binding of p27^{kip1} to RhoA. If p27^{kip1} is essential for p27RF-Rho to regulate RhoA activation, the absence of p27^{kip1} should abolish regulation of RhoA by p27RF-Rho. Knockdown of p27^{kip1} using siRNA increased the amount of GTP-RhoA by 1.6-fold (Fig. 4*A*, *a* for Western blots and Fig. 4*A*, *b* for quantification), consistent with a negative role for p27^{kip1} in RhoA activation as reported previously (12, 23–25). Expression of p27RF-V5 in the knockdown cells did not augment RhoA activation any further (Fig. 4*A*, *a* and *b*).

Cellular activation of RhoA can be induced by various external stimulants such as LPA, phorbol 12-myristate 13-acetate,

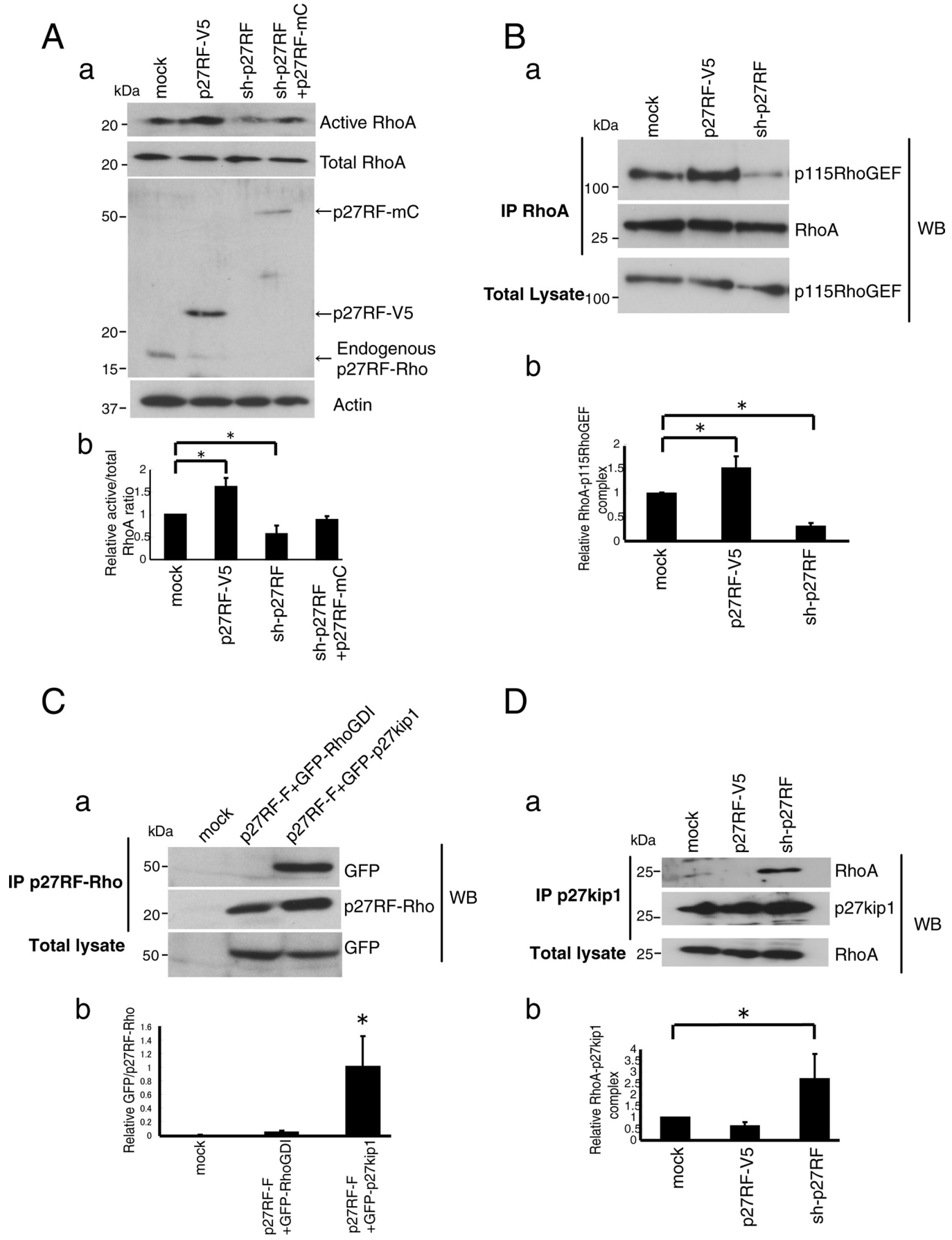
A
a
kDa
mock
p27RF-V5
sh-p27RF
sh-p27RF +p27RF-mC
20
Active RhoA
20
Total RhoA
50
←p27RF-mC
←p27RF-V5
20
15
← Endogenous p27RF-Rho
37
Actin
b
Relative active/total RhoA ratio
mock
p27RF-V5
sh-p27RF
sh-p27RF +p27RF-mC
B
a
kDa
mock
p27RF-V5
sh-p27RF
IP RhoA
100
p115RhoGEF
25
RhoA
WB
Total Lysate
100
p115RhoGEF
b
Relative RhoA-p115RhoGEF complex
mock
p27RF-V5
sh-p27RF
C
a
kDa
mock
p27RF-F+GFP-RhoGDI
p27RF-F+GFP-p27kip1
IP p27RF-Rho
50
GFP
20
p27RF-Rho
WB
Total lysate
50
GFP
b
Relative GFP/p27RF-Rho
mock
p27RF-F +GFP-RhoGDI
p27RF-F +GFP-p27kip1
D
a
kDa
mock
p27RF-V5
sh-p27RF
IP p27kip1
25
RhoA
25
p27kip1
WB
Total lysate
25
RhoA
b
Relative RhoA-p27kip1 complex
mock
p27RF-V5
sh-p27RF

and FBS. Indeed, the amount of GTP-RhoA increased upon treatment of the cells with these compounds (Fig. 4*B*, *a* for Western blots and Fig. 4, *B*, *b* for quantification). However, down-regulation of endogenous p27RF-Rho significantly suppressed the increase in GTP-RhoA, although this suppression was not complete (Fig. 4*B*, *a* and *b*). Stimulation of the cells with LPA or FBS also increased association of endogenous p27RF-Rho with endogenous p27^{kip1} in the cells (Fig. 4*C*, *a* and *b*).

Based on the results presented in Figs. 3 and 4, we propose a role for p27RF-Rho in the activation of RhoA as summarized in Fig. 4*D*. Activation of RhoA can be inhibited by p27^{kip1} as reported previously (12, 23–25). p27RF-Rho binds p27^{kip1} so as to free it from GDP-RhoA and thereby renders GDP-RhoA accessible to GEFs that mediates GDP-GTP exchange.

Co-localization of p27RF-Rho with Active RhoA and Punctate Actin Expression after Cell Stimulation—Stimulation of HT1080 cells with LPA induced activation of RhoA and enhanced the polymerization of actin (Fig. 2*B*). p27RF-Rho detected by an anti-p27RF-Rho polyclonal antibody exhibited a punctate distribution and did not show any clear co-localization pattern with actin in non-stimulated cells (Fig. 5*A*, *c*). The expression signals were specific to p27RF-Rho, as knockdown of p27RF-Rho expression abolished the signals almost completely (Fig. 5*A*, *h* and *k*). The punctate distribution of p27RF-Rho expression was not affected after treatment of cells with LPA (Fig. 5*A*, *e*). Upon stimulation of the cells, stress fibers and punctate actin structures became apparent (Fig. 5*A*, *d*). The punctate pattern of p27RF-Rho expression was observed to largely overlap with that of actin in LPA-treated cells (Fig. 5*A*, *f*), although co-localization of p27RF-Rho with the stress fibers was not apparent. When cells whose endogenous p27RF-Rho had been knocked down were treated with LPA, the actin structure at the sites of membrane ruffling became more prominent than either stress fibers or actin dots (Fig. 5*A*, *j*).

Next, GTP-loaded Rho subfamily members including RhoA were visualized in the cells by treating fixed cell samples with purified GST-RBD and then with an anti-GST antibody (26, 27). GST treatment alone did not produce significant signals within the cells (not shown). Active RhoA was observed weakly within the serum-starved cells (Fig. 5*B*, *b*), and stimulation of the cells with LPA generally enhanced the signal (Fig. 5*B*, *f*), leading to the appearance of an enhanced punctate morphology within a fraction of this signal. Within the same cell, the punctate p27RF-Rho signal (Fig. 5*B*, *e*, *green*) overlapped with that of both GST-RBD (Fig. 5*B*, *f*, *red*) and actin (Fig. 5*B*, *g*, *blue*). Co-localization of the three signals appears as white punctate structures within the merged image (Fig. 5*B*, *h*).

We also evaluated localization of cortactin, which is a regulator of actin polymerization and a marker for invadopodia (Fig. 6*A*, *a*). Corresponding to the formation of punctate actin structure at sites of p27RF-Rho localization, we observed most of p27RF-Rho patches co-localized with cortactin (Fig. 6*A*, *a* and *b*).

Then we examined whether MT1-MMP co-localizes with p27RF-Rho. MT1-MMP localized to the ruffling membrane at the cell periphery (Fig. 6*A*, *c*, *open arrowhead*) and in the region surrounding the nucleus in a punctate pattern of distribution (Fig. 6*A*, *c*). Some of the perinuclear dots may correspond to the protein within the Golgi complex. However, some MT1-MMP signals and punctate p27RF-Rho signals overlapped one another. We observed that ~30% of the punctate p27RF-Rho signals overlapped with MT1-MMP (Fig. 6*B*). The cells were next cultured on fluorescently labeled gelatin, and the proteolytic activity of MT1-MMP was visualized as *dark spots* (Fig. 6*C*, *c*). A confocal image of the gelatin layer (Fig. 6*C*, *d*, X-Y section) and X-Z images of MT1-MMP, p27RF-Rho, and gelatin are presented (Fig. 6*C*, *d*, *right panels*). The punctate p27RF-Rho signal extended into the gelatin layer, and the cellular protrusions overlapping the area of MT1-MMP expression showed evidence of gelatin degradation.

Membrane Targeting of p27RF-Rho Is Critical for the Generation of the Punctate Pattern of Actin Distribution—p27RF-Rho contains potential lipid modification sites; that is, one myristoylation and two palmitoylation sites at the N terminus (Fig. 7*A*, NH_2-MGCCY). We generated p27RF-Rho mutants with mutations at these sites (Fig. 7*A*, MASSY) and a revertant with seven amino acids added to the N terminus of the mutant (*Nrev*) (Fig. 7*A*). To examine whether p27RF-Rho associates with the plasma membrane, wild type or mutant p27RF-Rho was expressed in HT 1080 cells as V5-tagged forms. The cells were then disrupted under low osmotic pressure, subdivided into membrane and cytoplasmic fractions, and subjected to Western blot analysis (Fig. 7*B*). Transferrin receptor and tubulin were monitored as markers of membrane and cytoplasmic proteins, respectively. Wild type p27RF-Rho detected with anti-V5 antibody was mostly distributed to the membrane fraction, whereas a small fraction of the signal was detected in the cytoplasm. The amount of mutant p27RF-Rho (ASS) detected in the membrane fraction was greatly reduced compared with that of the wild type protein, whereas the amount detected in the cytoplasm was increased (Fig. 7*B*, *ASS* in the membrane fraction). Revertant p27RF-Rho showed a similar distribution pattern to that of the wild type protein (Fig. 7*B*, *Nrev*).

p27RF-Rho co-localized with MT1-MMP (Fig. 6), and immunoprecipitation of each protein co-immunoprecipitated the other (Fig. 1*B*). To evaluate the importance of the membrane-targeting signals of p27RF-Rho for this association with MT1-MMP, we expressed wild type and mutant p27RF-Rho as

FIGURE 3. **p27RF-Rho promotes the association of GEFs with RhoA.** *A*, GTP-loaded Rho proteins in HT1080 cell lysate were pulled down using GST-Rhotekin for RhoA. RhoA proteins were analyzed by Western blot (*WB*) using specific antibodies (*a*, *upper panel*). Quantification of active RhoA normalized to total RhoA (*b*, $n = 3$). *, $p < 0.05$ (Student's *t* test). Endogenous and exogenous p27RF-Rho proteins were detected with an anti-p27RF-Rho polyclonal antibody (*a*, *middle panel*). *B*, *a*, the effect of p27RF-Rho on the association of Myc-RhoA with V5-p115RhoGEF was tested. Myc-RhoA was immunoprecipitated (*IP*) and the associated GEFs were detected by Western blot analysis. *b*, quantification of Fig. 2*B*, *a* ($n = 3$). *, $p < 0.05$ (Student's *t* test). *C*, *a*, GFP-RhoGDI or GFP-p27^{kip1} was expressed together with p27RF-F in HT1080 cells. p27RF-F was immunoprecipitated using an anti-FLAG antibody, and associated GFP-fused proteins were detected by Western blot assay using an anti-GFP antibody. A representative result of three experiments is indicated. *b*, quantification of *C*, *a* ($n = 3$). *, $p < 0.05$ (Student's *t* test). *D*, *a*, Myc-RhoA and FLAG-p27^{kip1} were expressed in HT1080 cells expressing either p27RF-V5 or sh-p27RF. FLAG-p27^{kip1} was immunoprecipitated, and Myc-RhoA was detected in the precipitates by Western blot analysis. *b*, quantification of Fig. 2*D*, *a* ($n = 3$). *, $p < 0.05$ (Student's *t* test).

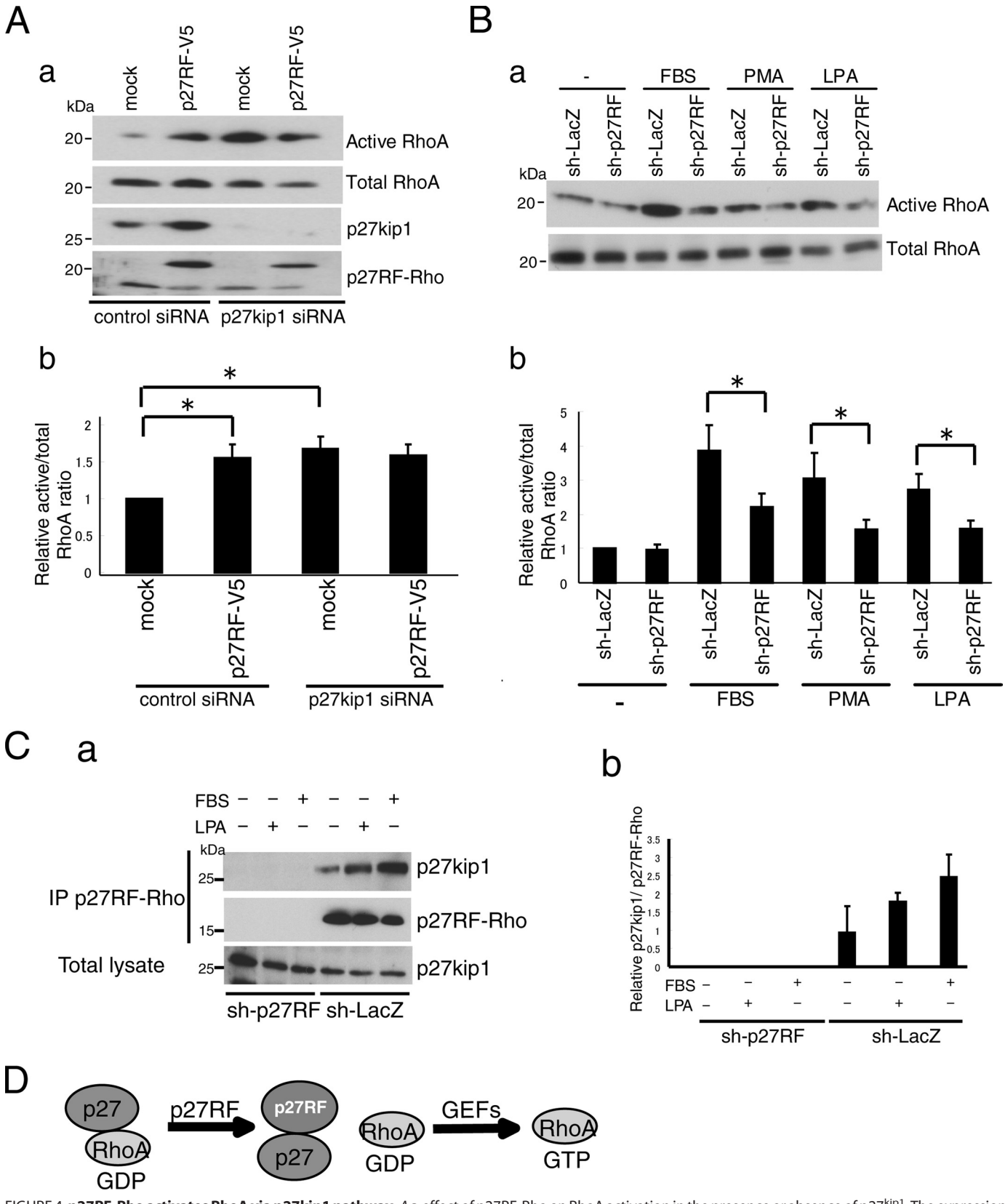

FIGURE 4. **p27RF-Rho activates RhoA via p27kip1 pathway.** *Aa*, effect of p27RF-Rho on RhoA activation in the presence or absence of p27^{kip1}. The expression of p27^{kip1} in HT1080 cells was knocked down using siRNA. *b*, quantification of the ratio of active RhoA to total RhoA ($n = 3$). *, $p < 0.05$ (Student's *t* test). *B*, *a*, HT1080 cells were serum-starved and treated with FBS, phorbol 12-myristate 13-acetate (*PMA*), or LPA in the presence or absence of sh-p27RF, and active RhoA was detected. *b*, quantification of the Western blots ($n = 3$). *, $p < 0.05$ (Student's *t* test). *C*, *a*, HT1080 cells were serum-starved and treated with LPA or FBS, then p27^{kip1} immunoprecipitated (*IP*) using anti-p27RF-Rho antibody. sh-p27RF was a negative control. *b*, quantification of *C*, *a* ($n = 3$). *D*, schematic illustration of the role of p27RF-Rho in the activation of RhoA. p27 ^{kip1} binds GDP-RhoA and prevents GDP-RhoA from binding GEFs. p27RF-Rho binds p27 ^{kip1} and sequesters the latter from GDP-RhoA. GDP-RhoA free from p27 ^{kip1} can be activated by associating with GEFs.

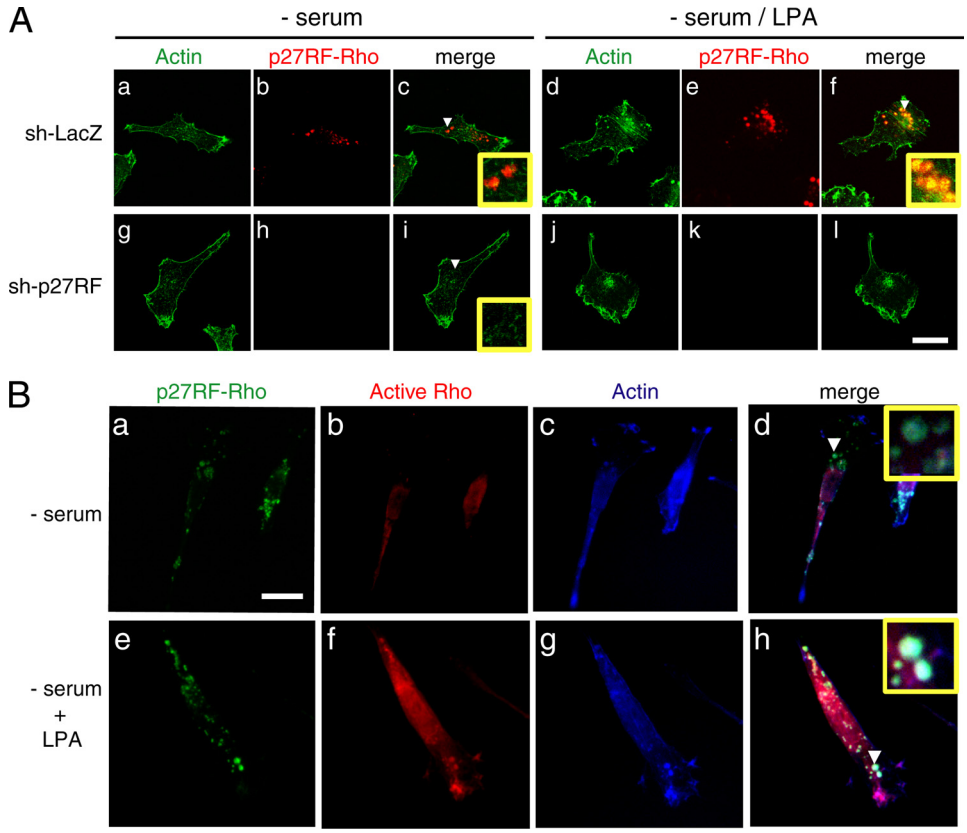

FIGURE 5. **Co-localization of p27RF-Rho, active RhoA, and actin.** *A*, HT1080 cells expressing sh-p27RF or sh-LacZ were seeded onto collagen-coated glass coverslips. Cells were serum-starved and treated with LPA. Actin was visualized with Alexa488-phalloidin (*green*), and p27RF-Rho was visualized with anti-p27RF-Rho (*red*). The area indicated by the *white arrowhead* is magnified in the *inset*. Confocal images were performed using a 63× objective lens (*scale bar*, 20 μm). *B*, after fixation the cells were incubated with soluble GST-RBD to detect active RhoA. Bound GST-RBD was visualized by immunostaining using anti-GST antibody (*red*). The same samples were double-stained for p27RF-Rho (*green*) and actin (*blue*). The area indicated by the *white arrowhead* is magnified in the *inset*. CCD images were performed using a 60× objective lens (*scale bar*, 20 μm).

FLAG-tagged forms in HT1080 cells and analyzed them by immunoprecipitation followed by Western blot analysis to detect MT1-MMP (Fig. 7*C*, *a*). MT1-MMP was detected in the precipitate of p27RF-F (wild type). In contrast, the ASS mutant protein failed to co-precipitate MT1-MMP. Nrev p27RF-F, which associated with the plasma membrane, restored the ability to co-precipitate MT1-MMP. However, the transferrin receptor used as a membrane protein control was not co-precipitated with p27RF-F. Thus, association of p27RF-Rho with the plasma membrane is mediated by the N-terminal amino acid sequence, and it is important for the protein interaction with MT1-MMP.

Immunostaining of cells treated with LPA revealed that p27RF-mC showed a punctate distribution (Fig. 7*D*, *c*, *WT*) as demonstrated for the endogenous proteins in Fig. 5*A*, *a* and *d*. However, p27RF-mC containing the ASS mutation largely failed to exhibit this punctate pattern of distribution and instead appeared to be distributed diffusely throughout the cell (Fig. 7*D*, *g*), whereas the Nrev mutation restored the punctate pattern of distribution observed for the wild type protein (Fig. 7*D*, *k*). Formation of punctate actin structures was also observed in cells expressing the ASS mutant p27RF-mC because the cells express endogenous p27RF-Rho. Only wild type and Nrev p27RF-mC showed co-localization with actin and cortactin within the punctate cell structures, which are indicated by the white areas where the three fluorescent signals overlap with each other (Fig. 7*D*, *d* and *l*). The ability of the mutant p27RF-Rho to promote cellular invasion into Matrigel was analyzed by expressing the mutant proteins in cells in which the endogenous p27RF-Rho had been down-regulated by shRNA expression (Fig. 7*E*). Expression of p27RF-mC and Nrev-mC but not the mutant (ASS-mC) restored the invasion-promoting activity (Fig. 7*F*).

DISCUSSION

The present study has identified a new system regulating the activation of RhoA mediated by p27RF-Rho, a newly discovered $p27^{kip1}$-binding protein. The binding of p27RF-Rho to $p27^{kip1}$ sequesters $p27^{kip1}$ away from GDP-RhoA and releases the latter in a form accessible to GEFs for GDP-GTP exchange, as summarized in supplemental Fig. S1*A*. Based on this mechanism, localization of p27RF-Rho appears to be important for defining the subcellular region where GDP-RhoA can be activated by GEFs in response to stimuli as summarized in supplemental Fig. S1, *A* and *B*). Indeed, p27RF-Rho co-localized with active RhoA within punctate cellular structures that contained actin in HT1080 cells treated with LPA (Fig. 7*B*). p27RF-Rho was identified as a protein associating with MT1-MMP. However, it is of note that the activity of p27RF-Rho was not affected significantly by the presence or absence of MT1-MMP.

Regulation of the Formation of Punctate Subcellular Structures Containing Actin by p27RF-Rho—Invasive cells frequently form invadopodia when the cells are cultured on ECM-coated glass slides, and the formation of these structures has been reported to correlate with the invasive ability of the cell (28). Invadopodia have been characterized as membrane protrusions with ECM-degrading proteases and cell adhesion molecules on their outer surface and an actin-based structure inside (29, 30). The protein p27RF-Rho we characterized in the present study regulates formation of punctate actin structures within the cells and a fraction of such punctate actin structures co-localized with MT1-MMP (Figs. 6 and 7*D*). The punctate distribution of p27RF-Rho expression co-localized well with that of actin and cortactin. However, only 30% of these punctate signals co-localized with MT1-MMP expression. Punctate p27RF-Rho signals were observed to extend into cellular protrusions that invaded into the gelatin layer, and gelatin degradation was observed at those cellular protrusions characterized

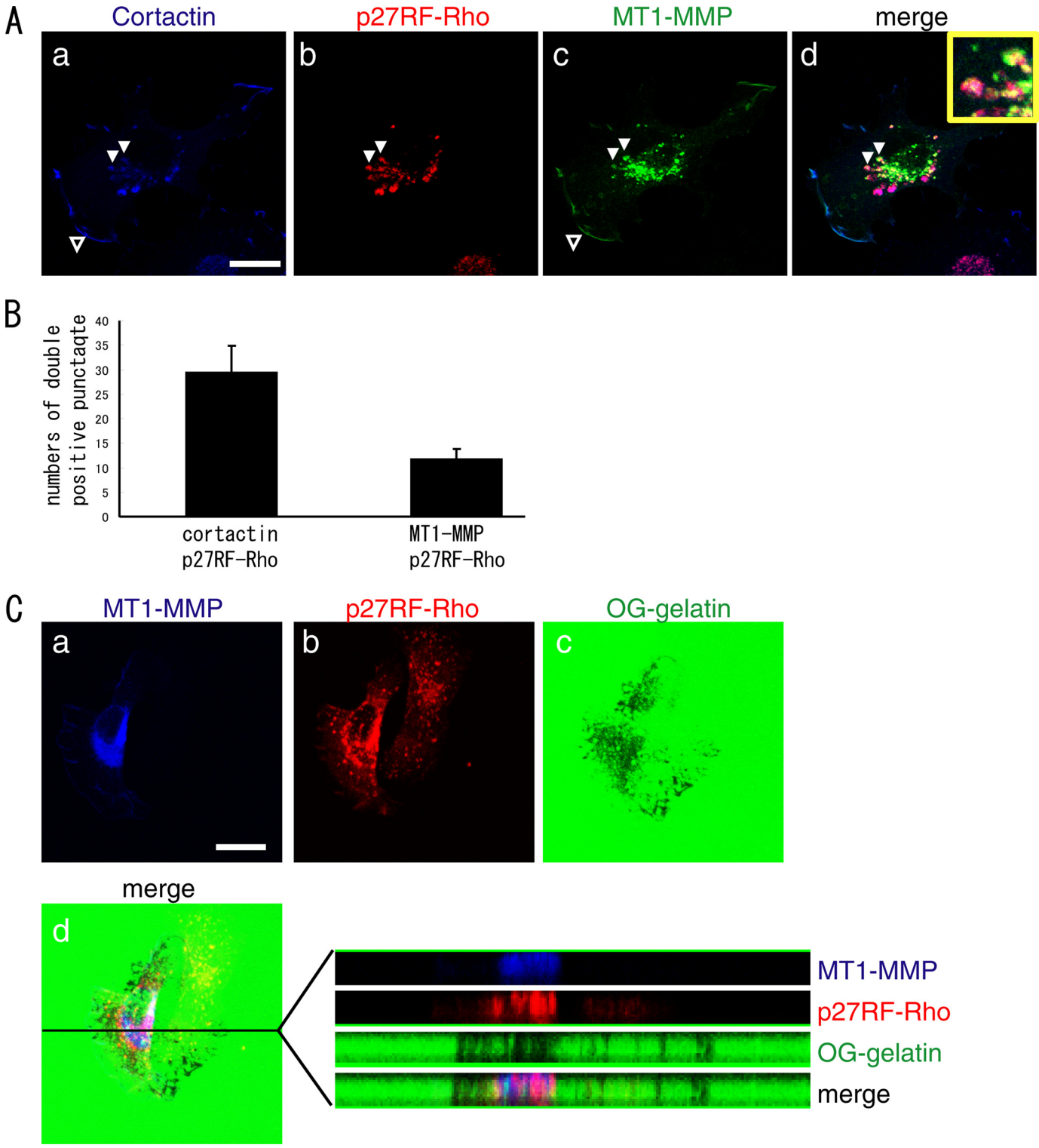

FIGURE 6. **p27RF-Rho co-localized with MT1-MMP.** *A*, MT1-MMP with a C-terminal Venus-tag was expressed in HT1080. The cells were stained for MT1-MMP (*green*), p27RF-Rho (*red*), and cortactin (*blue*). The area indicated by the *white arrowhead* is magnified in the *inset*. Confocal images used a 63× objective lens (*scale bar*, 20 μm). *B*, the number of punctate p27RF-Rho signals or MT1-MMP-p27RF-Rho double positive punctate signals were counted. Data are the mean ± S.D. ($n = 3$). *C*, *a–d*, HT1080 cells cultured on Oregon Green-labeled gelatin-coated glass coverslips. After fixation, the cells were stained for p27RF-Rho (*red*) and MT1-MMP (*blue*). Note that the degradation of gelatin is specific to the cells expressing exogenous MT1-MMP. *d*, X-Y and X-Z sections of the gelatin layer and merged image. Confocal images were performed using a 63× objective lens (*scale bar*, 20 μm).

by overlapping MT1-MMP expression (Fig. 6*C*, *d*). These protrusions are most likely invadopodia, which are actin-based cell protrusions that exhibit ECM degrading activity. Thus, MT1-MMP appears to be recruited to the punctate actin structures at a later stage so as to form mature invadopodia. Stimulation of HT1080 cells with LPA induced the formation of actin dots including invadopodia-like actin structures. Knockdown of p27RF-Rho in the cells prevented formation of these structures

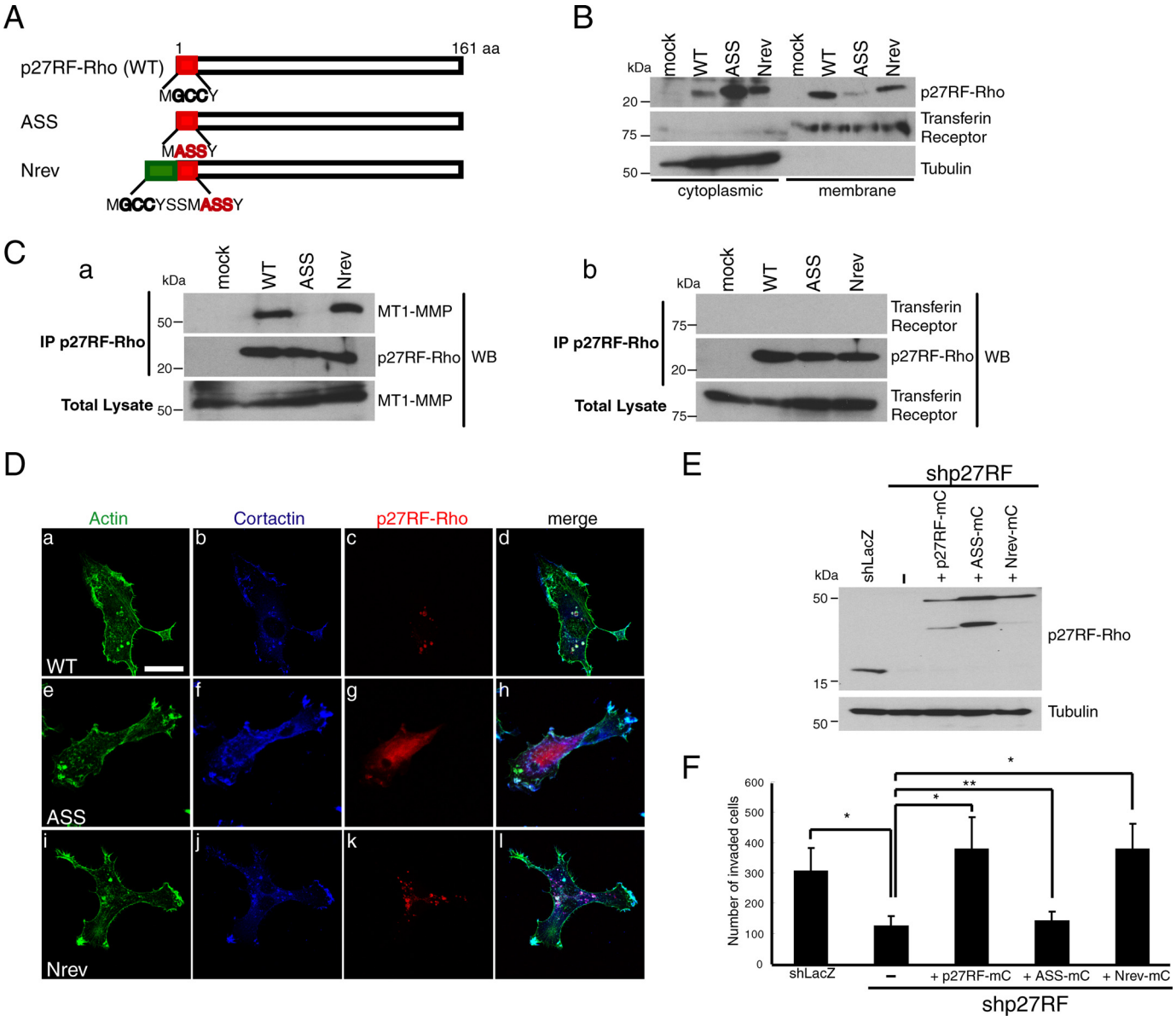

FIGURE 7. **Membrane targeting signals of p27RF-Rho are necessary to localize to the punctate actin structures and bind to MT1-MMP.** *A*, N-terminal sequences of p27RF-Rho, and its mutants are presented. Gly and Cys indicated by *black bold letters* correspond to hypothetical myristoylation and palmitoylation sites, respectively. *ASS*, acylation defective mutant; *Nrev*, additional acylation sites were fused to the N terminus of the ASS mutant. *B*, the following proteins were expressed in HT1080 cells; mock (empty vector), wild type (*WT*), ASS, and Nrev. After cells were lysed and separated into cytoplasmic and membrane fractions, p27RF-Rho was detected by Western blot analysis. Transferrin receptor and tubulin are representative makers for membrane and cytoplasmic proteins, respectively. A representative result of three experiments is indicated. *C*, Myc-tagged-MT1-MMP (*a*) and hemagglutinin-tagged transferrin receptor (*b*) were expressed together with p27RF-F or its mutants in HT1080 cells. The cells were lysed, and p27RF-F was immunoprecipitated (*IP*) using an anti-FLAG antibody. p27RF-Rho and its mutants bound to the antibody were eluted with FLAG peptides and subjected to Western blot (*WB*) analysis using anti-Myc or anti-HA antibodies. A representative result of three experiments is indicated. *D*, p27RF-Rho and its mutant proteins fused to an mCherry tag were expressed in HT1080 cells, and the cells were seeded onto collagen-coated glass coverslips, then serum-starved and treated with LPA. After fixation, the cells were stained for mCherry (*red*), cortactin (*blue*), and actin (*green*). Confocal images were performed using a 63× objective lens (*scale bar*, 20 μm). *E* and *F*, effect of mutant p27RF-Rho on Matrigel invasion. Expression of endogenous p27RF-Rho was knocked down using shRNA in HT1080 cells, and mutant p27RF-Rho proteins were expressed. Proteins were analyzed by Western blot analysis (*E*). The invasive activity of the cells was analyzed using a Transwell Chamber equipped with a Matrigel-coated filter, and the number of invaded cells was counted. Data are presented as the mean ± S.D. ($n = 3$). *, $p < 0.05$ (Student's *t* test).

(Fig. 5*A*) and diminished the invasive activity of the cell (Fig. 2*B*). Thus, it is of particular interest whether and how p27RF-Rho regulates the formation and turnover of invadopodia.

The subcellular localization of p27RF-Rho showed a punctate distribution pattern even before stimulation of the cells, and the pattern resembled that of the actin dots formed in response to cell stimulation. Thus, the localization of p27RF-Rho appears to determine the subcellular region where external signals are transmitted to activate RhoA and induce actin polymerization. The question of how p27RF-Rho localizes to particular patches of the plasma membrane remains unanswered, and we are trying to identify membrane proteins that interact with p27RF-Rho to understand the mechanism. It is interesting that p27RF-Rho associated with the plasma membrane fraction (Fig. 7*B*) co-precipitated MT1-MMP in an immunoprecipitation assay (Fig. 7*C*), whereas a mutant

p27RF-Rho lacking acylation sites that fails to associate with the membrane fraction did not. However, direct interaction between the cytoplasmic tail of MT1-MMP and p27RF-Rho was not detected at least *in vitro* (not shown). Thus, we suppose that MT1-MMP and p27RF-Rho are co-assembled into a multiprotein complex in invasion-related structures such as invadopodia.

Association of p27RF-Rho with Plasma Membrane—p27RF-Rho has its own intrinsic mechanism for localizing to the plasma membrane as revealed by biochemical fractionation and sequence manipulation of p27RF-Rho (Fig. 7, *A* and *B*). Three potential acylation sites exist in the N-terminal region of p27RF-Rho. Mutation of the three sites (ASS) greatly diminished the amount of the protein in the membrane fraction, whereas fusion of additional modification sites to the N terminus of the mutant restored the protein to the membrane fraction. Thus, p27RF-Rho has an intrinsic mechanism for localizing to sites of activation of RhoA by GEFs (supplemental Fig. S1). Because knockdown of p27RF-Rho significantly reduced activation of RhoA in response to stimuli, we think p27RF-Rho is an important player regulating transmission of different types of signals to activate RhoA. RhoA is important for a variety of cellular functions (10, 16, 31). Presumably p27RF-Rho does not universally mediate all processes that regulate RhoA. For example, we have not observed any effect of p27RF-Rho on cell division where cytokinesis of the duplicated cells is regulated by RhoA (32).

RhoA plays crucial roles in many diseases, including cancer, arteriosclerosis, and neuronal diseases (33, 34). Therefore, p27RF-Rho presents a promising new target to control RhoA activation and develop therapeutic agents for treating diseases associated with aberrant RhoA activity.

Acknowledgments—We thank Drs. N. Egawa and T. Sakamoto for useful discussion and Dr. R. Whittier for manuscript editing.

REFERENCES

1. Egeblad, M., and Werb, Z. (2002) *Nat. Rev. Cancer* **2,** 161–174
2. Itoh, Y., and Seiki, M. (2006) *J. Cell. Physiol.* **206,** 1–8
3. Overall, C. M., and Dean, R. A. (2006) *Cancer Metastasis Rev.* **25,** 69–75
4. Mori, H., Tomari, T., Koshikawa, N., Kajita, M., Itoh, Y., Sato, H., Tojo, H., Yana, I., and Seiki, M. (2002) *EMBO J.* **21,** 3949–3959
5. Weaver, A. M. (2008) *Curr. Biol.* **18,** R362–R364
6. Sakurai-Yageta, M., Recchi, C., Le Dez, G., Sibarita, J. B., Daviet, L., Camonis, J., D'Souza-Schorey, C., and Chavrier, P. (2008) *J. Cell Biol.* **181,** 985–998
7. Nakahara, H., Howard, L., Thompson, E. W., Sato, H., Seiki, M., Yeh, Y., and Chen, W. T. (1997) *Proc. Natl. Acad. Sci. U.S.A.* **94,** 7959–7964
8. Tomari, T., Koshikawa, N., Uematsu, T., Shinkawa, T., Hoshino, D., Egawa, N., Isobe, T., and Seiki, M. (2009) *Cancer Sci.* **100,** 1284–1290
9. Bishop, A. L., and Hall, A. (2000) *Biochem. J.* **348,** 241–255
10. Sahai, E., and Marshall, C. J. (2002) *Nat. Rev. Cancer* **2,** 133–142
11. McAllister, S. S., Becker-Hapak, M., Pintucci, G., Pagano, M., and Dowdy, S. F. (2003) *Mol. Cell. Biol.* **23,** 216–228
12. Besson, A., Gurian-West, M., Schmidt, A., Hall, A., and Roberts, J. M. (2004) *Genes Dev.* **18,** 862–876
13. Besson, A., Dowdy, S. F., and Roberts, J. M. (2008) *Dev. Cell* **14,** 159–169
14. Uekita, T., Gotoh, I., Kinoshita, T., Itoh, Y., Sato, H., Shiomi, T., Okada, Y., and Seiki, M. (2004) *J. Biol. Chem.* **279,** 12734–12743
15. Sato, H., Takino, T., Okada, Y., Cao, J., Shinagawa, A., Yamamoto, E., and Seiki, M. (1994) *Nature* **370,** 61–65
16. Ridley, A. J. (2001) *J. Cell Sci.* **114,** 2713–2722
17. Tsuji, T., Ishizaki, T., Okamoto, M., Higashida, C., Kimura, K., Furuyashiki, T., Arakawa, Y., Birge, R. B., Nakamoto, T., Hirai, H., and Narumiya, S. (2002) *J. Cell Biol.* **157,** 819–830
18. Pinner, S., and Sahai, E. (2008) *Nat. Cell Biol.* **10,** 127–137
19. Gadea, G., de Toledo, M., Anguille, C., and Roux, P. (2007) *J. Cell Biol.* **178,** 23–30
20. Abécassis, I., Olofsson, B., Schmid, M., Zalcman, G., and Karniguian, A. (2003) *Exp. Cell Res.* **291,** 363–376
21. Marinissen, M. J., Chiariello, M., Tanos, T., Bernard, O., Narumiya, S., and Gutkind, J. S. (2004) *Mol. Cell* **14,** 29–41
22. Olofsson, B. (1999) *Cell. Signal.* **11,** 545–554
23. Wu, F. Y., Wang, S. E., Sanders, M. E., Shin, I., Rojo, F., Baselga, J., and Arteaga, C. L. (2006) *Cancer Res.* **66,** 2162–2172
24. Papakonstanti, E. A., Ridley, A. J., and Vanhaesebroeck, B. (2007) *EMBO J.* **26,** 3050–3061
25. Lee, S. A., Lee, S. Y., Cho, I. H., Oh, M. A., Kang, E. S., Kim, Y. B., Seo, W. D., Choi, S., Nam, J. O., Tamamori-Adachi, M., Kitajima, S., Ye, S. K., Kim, S., Hwang, Y. J., Kim, I. S., Park, K. H., and Lee, J. W. (2008) *J. Clin. Invest.* **118,** 1354–1366
26. Berdeaux, R. L., Díaz, B., Kim, L., and Martin, G. S. (2004) *J. Cell Biol.* **166,** 317–323
27. Sahai, E., Garcia-Medina, R., Pouysségur, J., and Vial, E. (2007) *J. Cell Biol.* **176,** 35–42
28. Monsky, W. L., Kelly, T., Lin, C. Y., Yeh, Y., Stetler-Stevenson, W. G., Mueller, S. C., and Chen, W. T. (1993) *Cancer Res.* **53,** 3159–3164
29. Gimona, M., Buccione, R., Courtneidge, S. A., and Linder, S. (2008) *Curr. Opin. Cell Biol.* **20,** 235–241
30. Weaver, A. M. (2006) *Clin. Exp. Metastasis* **23,** 97–105
31. Ridley, A. J., Schwartz, M. A., Burridge, K., Firtel, R. A., Ginsberg, M. H., Borisy, G., Parsons, J. T., and Horwitz, A. R. (2003) *Science* **302,** 1704–1709
32. Piekny, A., Werner, M., and Glotzer, M. (2005) *Trends Cell Biol.* **15,** 651–658
33. Fritz, G., and Kaina, B. (2006) *Curr. Cancer Drug Targets* **6,** 1–14
34. Ming, X. F., Barandier, C., Viswambharan, H., Kwak, B. R., Mach, F., Mazzolai, L., Hayoz, D., Ruffieux, J., Rusconi, S., Montani, J. P., and Yang, Z. (2004) *Circulation* **110,** 3708–3714